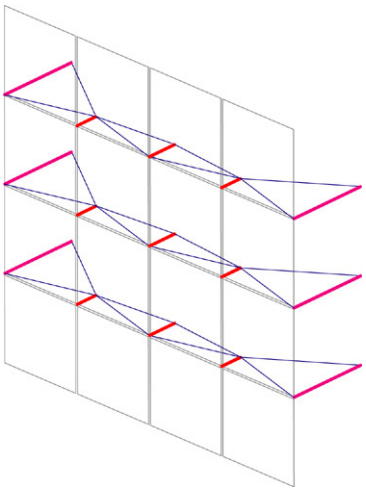

Fig. 6(b). Point-fixed glazing system: axonometric, scale 1.

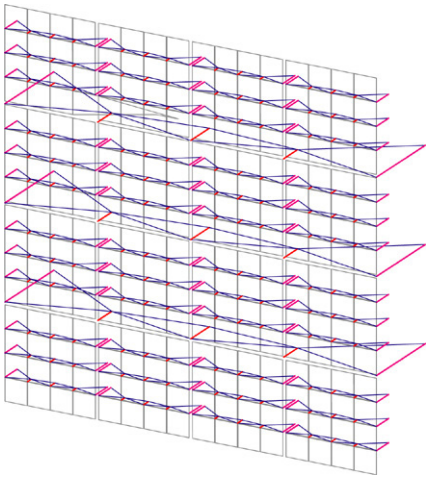

Fig. 6(c). Point-fixed glazing system: axonometric, scale 2.

supporting system, the static analysis and the progressive morphological subdivision of the structural components are important parameters in the generation of self-similarity. The dimensions of the various lines, as they are computed by the program, can be used in practice as dimensions of the various components of the structural system.

In order to examine whether the idea of the creation of an organized hierarchical process, by the use of the point fixed glazing systems, is possible in practice, an algorithm has been created that simulates an existing structure with a fractal hierarchy in its supporting system: the façade of a Serre at La Villette by P. Rice in Paris. The structural system of this building can be used as a model, and be applied to the shells, which are described further, or to other similar ones, Figs. 6(b) and 6(c) [25].

Therefore, these examples exploit a new design technique, which applies the idea of fractal geometry in 3-d structures. The geometrical configuration, the structural morphology and the hierarchical subdivision of the support system generate a new architectural expression [25–27].

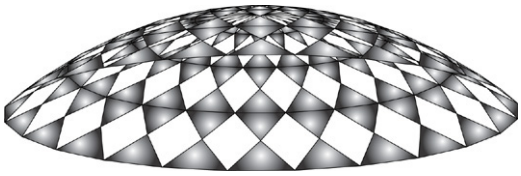

Fig. 7(a). Elliptic paraboloid.

4. The elliptic paraboloid and hyperbolic paraboloid shapes

To generate computerized fractal forms, geometric shapes have been used as a basis. Such examples are the elliptic paraboloid (e.p.) and the hyperbolic paraboloid (h.p.) shapes, Figs. 7(a) and 8(a) respectively. They are based on the following mathematical relations.

The e.p. and h.p. for the Euclidian space E^3 are respectively described by

$$\text{Elliptic paraboloid}: \frac{x^2}{a^2} + \frac{y^2}{\beta^2} - 2z = 0, \tag{5}$$

$$\text{Hyperbolic paraboloid}: \frac{x^2}{a^2} - \frac{y^2}{\beta^2} - 2z = 0. \tag{6}$$

The Cartesian coordinates x and y for a point on the surface of the e.p. or h.p., at a level

$z = z_0$ are given as

$$x = \alpha_j \cos(\theta \cdot i) \quad \text{and} \tag{7}$$

$$y = \beta_j \sin(\theta \cdot i). \tag{8}$$

where $i = 1, 2, \ldots$ Num_Points, and θ is the angle of rotation around the axis zz' [0°, 360°], which depends on the number of points (Num_Points) the user gives along a ring. A ring is every level z that subtracts, from the surface of the e.p. or h.p., a curve of the Euclidian space E^3. The user gives the number of rings (Num_Rounds)

$$\theta = \frac{2\pi}{\text{Num\_Points}} \quad \text{or} \quad \theta = \frac{360^\circ}{\text{Num\_Points}}. \tag{9}$$

The coefficients α_j and β_j represent the axes of the ellipse. The following relations give their values

$$\alpha_j = \alpha \frac{j}{\text{Num\_Rounds}} \tag{10}$$

$$\beta_j = \beta \frac{j}{\text{Num\_Rounds}}, \tag{11}$$

where $j = 1, 2, \ldots$ Num_Rounds
and α, β are the axes of the ellipse of the biggest ring, because for
$j =$ Num_Rounds then $\alpha_j \equiv \alpha$ and $\beta_j \equiv \beta$.
In the program, α is the value of Big Axial-A, and β is the value of Big Axial-B.
By substituting relations (9) and (10) into relations (7) and (8), the following coordinates are obtained

$$x = \alpha \cdot \left(\frac{j}{\text{Num\_Rounds}}\right) \cdot \cos(\theta \cdot i), \tag{12}$$

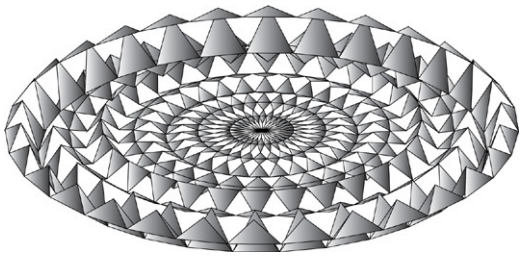

Fig. 7(b). Elliptic paraboloid with wave.

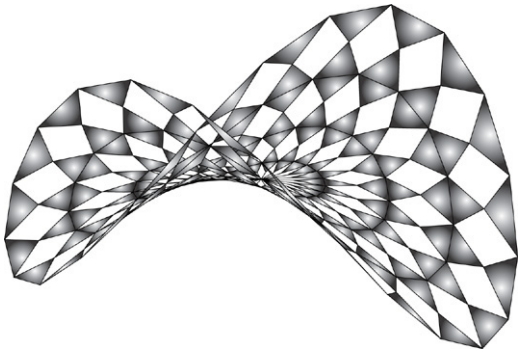

Fig. 8(a). Hyperbolic paraboloid.

$$y = \beta \cdot \left(\frac{j}{\text{Num\_Rounds}}\right) \cdot \sin(\theta \cdot i), \tag{13}$$

$$z = z_0. \tag{14}$$

The level z is written as

$$z = A\frac{\left(\frac{x^2}{a^2} + \frac{y^2}{\beta^2}\right)}{2}, \quad \text{for the e.p. and} \tag{15}$$

$$z = A\frac{\left(\frac{x^2}{a^2} - \frac{y^2}{\beta^2}\right)}{2}, \quad \text{for the h.p.} \tag{16}$$

The coefficient A is given by

$$A = B\sqrt{a^2 + \beta^2}, \tag{17}$$

where B is the scale factor of the axis zz' that produces different levels for the same axes α and β.

The complexity of the model can be increased if a variable equation is added in order to give a wave form along the axis zz'. The simple e.p. and h.p., Figs. 7(a) and 8(a), are transformed to fractal forms by the introduction of the angle of the wave. The height of the wave depends on the distance of the wave from the centre of the ellipse and on the number of periods along the axis of the ellipse, Fig. 7(b), 8(b) and 8(c). These shapes are similar to the waves created in water when a stone is thrown.

In this case, Eq. (17) is written as

$$A = B\sqrt{a^2 + \beta^2}\sin(\phi \cdot j), \tag{18}$$

where $j = 1, 2, \ldots,$ Num_Rounds.

Angle ϕ depends on the number of rings (Num_Rounds) and on the number of periods (Num_Periods) the user chooses to have along the total number of rings. Above every 2-rings of the original mesh, a parameterized height is added. These heights vary according to the following function:

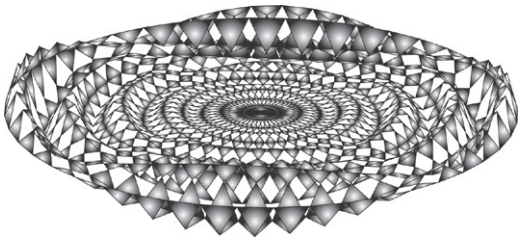

Fig. 8(b). Hyperbolic paraboloid with wave.

Fig. 8(c). Hyperbolic paraboloid with wave — Front view.

$$\phi = \frac{2\pi \cdot \text{Num\_Periods}}{\text{Num\_Rounds}}. \tag{19}$$

The coordinates x, y, z are obtained by combining Eqs. (12)–(18)

$$x = \alpha \cdot \left(\frac{j}{\text{Num\_Rounds}}\right) \cdot \cos(\theta \cdot i), \tag{20}$$

$$y = \beta \cdot \left(\frac{j}{\text{Num\_Rounds}}\right) \cdot \sin(\theta \cdot i), \tag{21}$$

$$z = B \cdot \sqrt{\alpha^2 + \beta^2} \cdot \left(\frac{j}{\text{Num\_Rounds}}\right)^2 \cdot \left(\frac{1}{2}\right) \cdot \sin(\phi \cdot j), \quad \text{for the e.p.} \tag{22}$$

or

$$z = B \cdot \sqrt{\alpha^2 + \beta^2} \cdot \left(\frac{j}{\text{Num\_Rounds}}\right)^2 \cdot \left(\frac{\cos^2(\theta \cdot i) - \sin^2(\theta \cdot i)}{2}\right) \cdot \sin(\phi \cdot j), \quad \text{for the h.p.,}$$

where $i = 1, 2, \ldots$ Num_Points, $j = 1, 2, \ldots$ Num_Rounds.

5. A tree on the surface of an elliptic paraboloid

In this section, the structural and geometrical transformation of the surface of an elliptic paraboloid based on a tree fractal configuration [28], Fig. 9, is studied. The evolution of the tree system generates two different models, depending on the rule that is applied for the development of the model. So e.g. factor 2* (relation (28)) and factor 2+ (relation (29)) give different results, as shown in Figs. 10 and 11 respectively. In order to produce the design representations of these 3-d shells, the following rules and mathematical formulas have been used:

As it has been described in the previous section, the elliptic paraboloid scheme is given by Eq. (5). On the above surface, a suitable number of points are chosen, so that a tree form is produced. To achieve this, the coordinates of the elliptic paraboloid are estimated in relation to the angle of rotation θ around the axis z, Eq. (9), and the number of levels z.

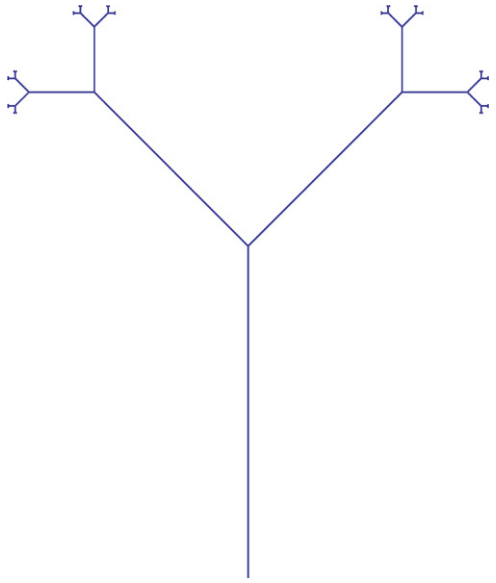

Fig. 9. Generation of the tree fractal.

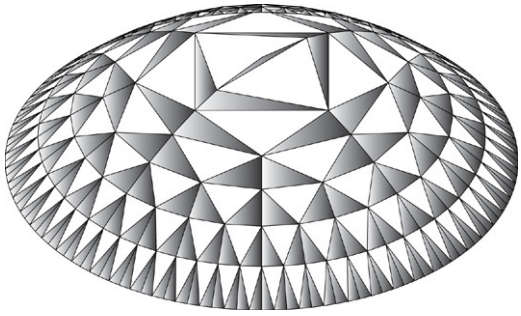

Fig. 10(a). Tree on the surface of an elliptic paraboloid. Model of geometrical progression.

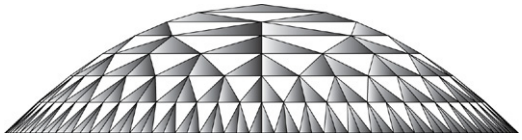

Fig. 10(b). Tree on the surface of an elliptic paraboloid. Model of geometrical progression — Front view.

The Cartesian coordinate z, that represents each time one ring (level z), is parameterized according to the number of rings (Num_Rounds) the user instructs the algorithm to develop, and is estimated by the paraboloid equation

$$z = a \cdot x^2 + b \cdot x + c, \quad \text{where } x \equiv i = 1, 2, \ldots, \text{Num\_Rounds}. \tag{23}$$

The user has to select the appropriate values for the coefficients a, b and c.

For a given value of the coordinate z (level z), which has been estimated by Eq. (23), and according to the equation of the elliptic paraboloid, Eq. (5), the parametric equations of the Cartesian coordinates x and y result in

$$x = \alpha_z \cos(\theta \cdot j) \quad \text{and} \tag{24}$$

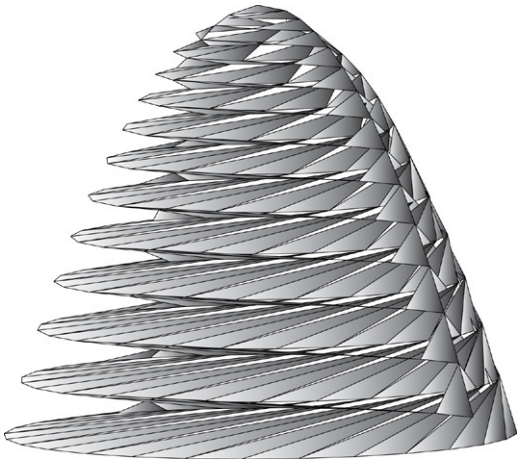

Fig. 11(a). Tree on the surface of an elliptic paraboloid. Model of arithmetical progression-Axonometric, view 1.

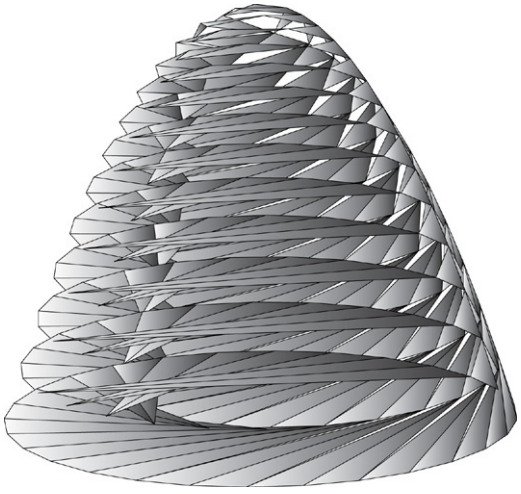

Fig. 11(b). Tree on the surface of an elliptic paraboloid. Model of arithmetical progression-Axonometric, view 2.

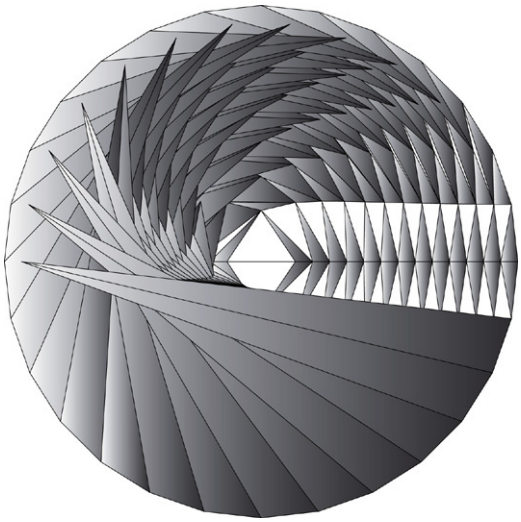

Fig. 11(c). Tree on the surface of an elliptic paraboloid. Model of arithmetical progression — View from below.

$$y = \beta_z \sin(\theta \cdot j), \tag{25}$$

where $j = 1, 2, \ldots,$ Num_Points.

On both the above relations, parameter θ is given as previously, Eq. (9).

The coefficients α_z and β_z represent the axes of the ellipse. Their values are given by the following functions

$$\alpha_z = \alpha \cdot \sqrt{2 \cdot |z|} \quad \text{and} \tag{26}$$

$$\beta_z = \beta \cdot \sqrt{2 \cdot |z|}, \tag{27}$$

where α_z and β_z are the axes of the ellipse of the ring whose $|z| = 1/2$, and thus $\alpha_z = \alpha$ and $\beta_z = \beta$. In the program, α is the value of Big Axial-A and β is the value of Big Axial-B, which are chosen by the user.

The user has also to select the "number of points on each ring". This parameter is different for each ring (level) and different models can describe the method of transformation. In the present case, the following models are chosen:

5.1. Model of geometrical progression, Figs. 10(a) and 10(b)

$$\text{Num\_Points}(i+1) = 2^{*}\text{Num\_Points}(i), \tag{28}$$

where $i = 1, 2, \ldots,$ Num_Rounds, with the following initial values

$$\text{Num\_Points}(0) = 1 \quad \text{and} \quad \text{Num\_Points}(1) = 2.$$

5.2. Model of arithmetical progression, Fig. 11

$$\text{Num\_Points}(i+1) = 2 + \text{Num\_Points}(i), \tag{29}$$

where $i = 1, 2, \ldots,$ Num_Rounds, with the following initial values

$$\text{Num\_Points}(0) = 1 \quad \text{and} \quad \text{Num\_Points}(1) = 2.$$

The coordinates x, y, z are obtained by combining Eq. (5) with Eqs. (24)–(27) and the following Eq. (32)

$$x = \alpha \cdot \sqrt{2 \cdot |a \cdot i^2 + b \cdot i + c|} \cdot \cos\left(\frac{2\pi}{\text{Num\_Points}} \cdot j\right), \tag{30}$$

$$y = \beta \cdot \sqrt{2 \cdot |a \cdot i^2 + b \cdot i + c|} \cdot \sin\left(\frac{2\pi}{\text{Num\_Points}} \cdot j\right), \tag{31}$$

$$z = \mathrm{a} \cdot i^2 + b \cdot i + c, \tag{32}$$

where $i = 1, 2, \ldots,$ Num_Rounds and $j = 1, 2, \ldots,$ Num_Points.

Fractal geometry is observed in the tree form of the surface. The more the number of rings is increased, the more subdivisions and points on each ring are taken (either by geometrical progression or by arithmetical progression). In Fig. 10, the number of points in each level is twice the number in the previous level. The triangles are similar in each level, and they can be either glass panels, or other materials with a steel frame system, or they can represent a reticulated supporting system as a point-fixed glazing system with cables. It must be noted that the model of geometrical progression is morphologically better than the model of arithmetical progression. The complex scheme of Fig. 11 could be a basis for a spiral building.

6. Conclusions

The new geometry, the geometry of Nature, has opened new routes in science, economics, urban-planning, biology etc. This geometry has recently influenced architecture also. The proposed computational method produces algorithms using fractal mathematics, and can generate forms applicable to shells. Modern building technology can support such applications, e.g. it has been applied for the construction of the glass roof of the atrium in the British Museum, where each different node and bar was constructed according to the dimensions given by a computer program [20].

Considering the development of recent technologies in design and building construction, and the introduction of complex new forms in the architectural design, a new architectural mode of expression is generated.

This new morphology is produced digitally, according to the algorithmic potential of software programs, the structural performance of the building materials, the support systems and users' demand. The applications of this method are unlimited, given the enormous capacities of computer technology, and the possibilities for form generation are stretched far beyond the limits of purely manual techniques. They are variable, since they are used either for the whole building design or for parts of the construction, e.g. the roof or the profile of a wing, the roofs of atria, the cladding of a façade, or space installations like pavilions, shelters, tents, domes etc., and in large-scale planning like the design of a plaza or small-scale design like the pattern of a pavement.

Therefore, this idea is used for further improvement of the design of shells and other larger scale projects that arise in architecture or the engineering sciences. The benefit of such an approach is that when an algorithm is suggested for a structure, then the whole project is analysed and determined in such a way that every rule it contains can be fully described — for example, the coordinates of each node, or the dimensions of each bar. The result is a spatial structure providing a system with technological coherence and aesthetic value, rather than merely an interesting prototype. The challenge for the architects and the engineers is to be inspired by the computer results, either by simplifying the undesirable complexity involved, or by using in their design small parts of the whole computer product, applicable in real projects, that can be realised using new materials and modern structural technology.

References

[1] Mandelbrot B. The fractal geometry of nature. New York: Freeman & Co; 1983.
[2] Peitgen HO, Saupe D. The science of fractal images. New York: Springer-Verlag; 1988.
[3] Artemiadis N. The geometry of fractals. Proceedings of the Academy of Athens 1988;63:479–500 [in Greek].
[4] Peitgen HO, Jürgens H, Saupe D. Fractals for the classroom. New York: Springer-Verlag; 1992.
[5] Ho MW. The new age of the organism. Architectural Design 1997; 67(9–10):44–51.
[6] Batty M, Longley P. The fractal city. Architectural Design 1997;67(9–10): 74–83.